JOURNAL OF APPLIED POLYMER SCIENCE VOL. 12, PP. 1151–1165 (1968)

Growth, Morphology, and Reinforcement Potential of Low Molecular Weight Crystals in Amorphous Polymeric Matrices

JACQUES R. JOSEPH,* JOHN L. KARDOS, and LAWRENCE E. NIELSEN, *Monsanto Company/Washington University, St. Louis, Missouri 63166*

Synopsis

The technique of *in situ* crystallization of low molecular weight organic compounds from amorphous polymers was evaluated as a method of fabricating composite materials. Two workable systems, styrene–acrylonitrile copolymer (SAN)–acetanilide and SAN–anthracene, were found and their phase diagrams determined. In both systems kinetic studies revealed that the maximum crystallization rate takes place at large degrees of supercooling and that below these temperatures the mechanism is diffusion-controlled. The temperature-dependent crystal morphologies were characterized with electron microscopy, which showed three distinctly different morphologies for both systems. From dynamic mechanical measurements, it appears that the elastic moduli of organic crystals are about the same as those of organic polymers in the glassy state, and that relatively little reinforcement took place under the particular crystallization conditions employed.

INTRODUCTION

In many cases it would be convenient to be able to make composite materials which could be fabricated at high temperatures as homogeneous melts from which a rigid reinforcing phase develops as the system is cooled down to the solid state. A possible way of achieving this goal would be to use mixtures of rigid amorphous polymers and low molecular weight organic compounds, which are soluble in the polymer at high (fabrication) temperatures and which become insoluble and crystallize out of the viscous melt as the temperature is lowered. Thus, the well-known difficulties of processing and fabricating filled systems, especially those containing fibrous fillers, would be avoided. In addition, such techniques offer the possibility of controlling crystal morphology and orientation to a degree not possible with conventional fabrication techniques involving the flow of filled polymer melts.

Mixtures of organic compounds and high polymers offer possible answers to a number of important scientific questions in addition to those mentioned above. (*1*) What is the mechanism and rate of crystal growth of

*Present address: Diamond Alkali Company, Deer Park, Texas.

organic compounds from viscous liquids? (*2*) What changes in morphology of the crystalline phase are possible? (*3*) What are the elastic moduli of small organic crystals? Do such crystals offer the possibility of acting as good reinforcing fillers in the same way as single crystal whiskers of inorganic materials?

Two workable systems have been found and their phase diagrams determined. Crystallization kinetics and crystal morphology have been determined under a variety of conditions for crystals grown from very viscous polymer melts. Dynamic mechanical properties of such two-component, two-phase systems have been measured. It appears that the elastic moduli of organic crystals, which are held together by van der Waal's forces, are about the same as the moduli of organic polymers in the glassy state rather than the higher moduli associated with inorganic single crystals.

EXPERIMENTAL

Criteria for System Selection

In choosing the polymer matrix and the low molecular weight (LMW) component to be selectively crystallized, the following criteria must be considered.

Transition Temperatures. The melting point, and in most cases the dissolution (fabrication) temperature, of the LMW component must be considerably above the glass transition temperature T_g of the polymer matrix for several reasons. First, crystallization cannot occur readily from the glassy state, diffusion being much too slow; second, a wide crystallization temperature range above T_g permits better control over the crystallization morphology; and, finally, the higher the melting point is above T_g, the lower will be the polymer viscosity, thus hastening the dissolution process.

Obviously, the dissolution temperature cannot exceed the degradation temperature of either the polymer matrix or the LMW component. The LMW component also must not be volatile at the dissolution temperature.

Solubility. At the fabrication (dissolution) temperature, the two components must be completely miscible. However, the solubility should decrease as the temperature is lowered so that the LMW component can crystallize. Ideally, the LMW component would be 100% soluble slightly above its melting point and insoluble at the T_g of the pure polymer.

Degree of Dissolved-Phase Interaction. Any type of chemical reaction between the dissolved components is certainly undesirable, since it would affect the matrix properties in addition to hindering the subsequent crystallization process. Any other strong interactions which would tend to induce crystallization in the polymer at the dissolution temperature should also be avoided.

Since solubility and chemical interaction data are practically nonexistent for systems of this type, a considerable number of combinations were screened by using differential thermal analysis (DTA). Styrene–acrylo-

TABLE I
Physical Constants of the Low Molecular Weight Compounds

Compound	Chemical formula	Molecular weight	Melting temperature, °C.	Boiling temperature, °C.	Density (20°C.), g./cc.
Acetanilide	$CH_3CONHC_6H_5$	135	113–114	307	1.21
Anthracene	$C_6H_4(CH_2)C_6H_4$	178	216	340	1.25

nitrile copolymer (SAN) was chosen as the matrix because of its good chemical stability, convenient T_g, and ability to remain amorphous under all conditions used. The SAN contained 26 wt.-% acrylonitrile and had a number-average molecular weight of about 60,000. DTA showed a T_g of 100–102°C. and a degradation temperature of about 280°C. for the pure copolymer. Of several possible LMW compounds (hereafter designated fillers), acetanilide and anthracene, whose physical constants are summarized in Table I, were chosen to combine with SAN, giving two model systems which fulfill the above criteria reasonably well.

Sample Preparation

A rotating hammer mill was used to grind the SAN pellets, along with Dry Ice to prevent softening, into a fine (80 mesh) powder. Both the SAN and filler powders were dried overnight at 80°C. under a slight vacuum. The filler and polymer powders were weighed out and mixed in proportions calculated from the densities to yield the desired volume fractions.

Two types of specimens were prepared. The first was a test-tube sample containing about 5 g. of powder mixture. The test tubes were heated in an oil bath for 4 hr. at 160°C. for the acetanilide and at 200°C. for the anthracene mixtures. (Anthracene is soluble slightly below its melting point.) Following complete dissolution the samples were quenched in liquid nitrogen to prevent crystallization and give a hard glassy solid solution. The high volume-fraction acetanilide samples were stored in liquid nitrogen since the glass transition temperature of the SAN was depressed below room temperature. At this point the samples were ready for use in determining the phase diagrams and the crystallization kinetics for both systems. The second type of sample was prepared solely for dynamic testing and will be described below.

Phase Diagrams

Phase diagrams of the two model systems were determined for use in guiding subsequent crystallization kinetics experiments. Each phase diagram consists of two curves: the glass transition curve where T_g of the polymer matrix is plotted against the volume fraction filler, and the solubility curve where the crystallization temperature is plotted versus the filler volume fraction still in solution after complete crystallization (equilibrium).

Glass Transition Curve. Seven acetanilide–SAN and five anthracene–SAN test-tube samples were prepared containing various filler volume fractions from 0 up to 0.3 and 0.2, respectively. At higher concentrations it was difficult to avoid crystallization during the quenching step. After quenching, a DTA scan was run on each sample to determine the glass transition temperature.

Solubility Curve. Several sets of test-tube samples containing dissolved volume fractions of 0.3 acetanilide and 0.2 anthracene were prepared. Each set of samples was immersed in an oil bath at a chosen temperature and allowed to crystallize isothermally. After 2–3 days of isothermal crystallization, the first sample of the set was quenched and its T_g measured with DTA. The remaining samples were allowed to remain in the bath for one more day, after which another sample was quenched and analyzed with DTA. This step was repeated until a constant equilibrium T_g was obtained. The amount of LMW material remaining in solution at the chosen crystallization temperature was determined from the equilibrium T_g value and the glass transition curve. The entire procedure was repeated for a range of crystallization temperatures and a solubility curve constructed for each system.

Bulk Crystallization Kinetics

Two sets of test-tube samples were prepared, one containing 0.3 volume fraction acetanilide and the other 0.2 volume fraction anthracene. The following procedure was used to determine the increase in crystallinity as a function of time at constant temperature.

Five samples were simultaneously immersed in a thermostatted oil bath at the desired crystallization temperature. At regular intervals one sample was removed and quenched in liquid nitrogen and its T_g determined with DTA. The volume fractions left in solution after each time interval were determined from the T_g curve, and the difference between these values and the initial volume fraction yielded the crystallized volume fraction or crystallinity.

Specimen Characterization

Electron Microscopy. The morphology of the crystallized phase was studied by electron microscopy. Samples crystallized at various temperatures were quenched in liquid nitrogen and fractured. Platinum–carbon replicas of the fracture surface were then made and examined in the microscope.

Dynamic Mechanical Measurements. Special samples were prepared for dynamic testing. A large excess of powder, mixed as previously described, was poured into a $4 \times {}^3/_8 \times {}^1/_{16}$ in. sandwich-type mold. A heating time of 1 hr. at 150°C. for acetanilide and 200°C. for anthracene was sufficient to dissolve the filler crystals in the polymer. The solution was then molded under 1000 psi to flash out the excess and remove voids. Subsequent quenching in liquid nitrogen caused severe cracking in the thin

specimens making them useless for dynamic testing. However, cold-water quenching gave crack-free samples and, at the same time, prevented crystallization.

After molding and quenching, the rectangular beam-shaped specimens were crystallized isothermally in a thermostatted oil bath for several days while still in the mold. Then, following a cold-water quench, each sample was removed from the mold and mounted on a freely oscillating torsion pendulum.[1] Damped oscillation curves were recorded at 1 cps throughout a wide temperature range beginning at 243°K. and extending through the transition of each sample.

RESULTS AND DISCUSSION

Phase Diagrams

Glass Transition (T_g) Curves. DTA curves for quenched samples of various anthracene concentrations are shown in Figure 1. A noticeable break in the slope occurs at T_g. As the dissolved filler volume fraction increases, the T_g break shifts to a lower temperature. Similar curves resulted for the acetanilide system.

The effect of dissolved filler on T_g is summarized by the data points in Figures 2 and 3 (T_g curve) for the acetanilide and anthracene systems, respectively. The solid lines are the result of fitting eq. (1)[2] to the data points

$$T_g = \frac{\alpha_p(1 - V_f)T_{gp} + \alpha_f V_f T_{gf}}{\alpha_p(1 - V_f) + \alpha_f V_f} \tag{1}$$

where f and p refer to the filler and pure polymer, respectively, V is the volume fraction, and α is the linear expansion coefficient. For SAN, $\alpha_p = 8.1 \times 10^{-5}$ °C.$^{-1}$ α_f, and T_{gf} are unknown and were adjusted to fit the data points. In the case of acetanilide $\alpha_f = 18 \times 10^{-5}$ °C.$^{-1}$ and $T_{gf} =$

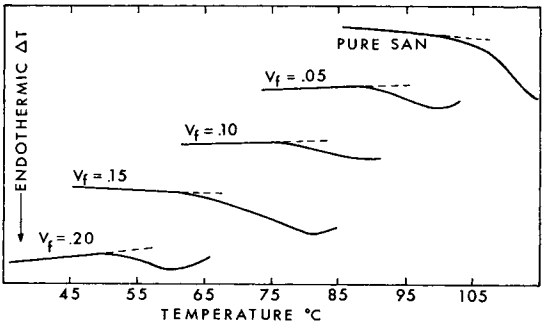

Fig. 1. DTA scans at 25°C./min. of the anthracene–SAN system at various volume fractions of dissolved filler (V_f), showing the lowering influence of the anthracene on the glass transition temperature.

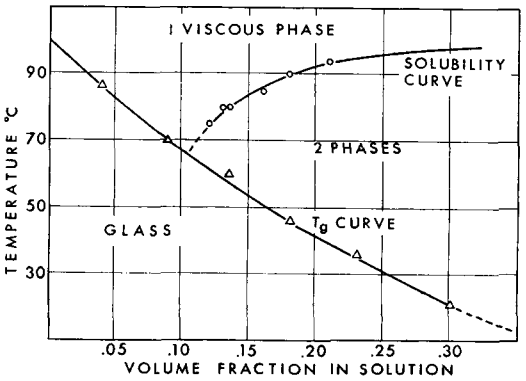

Fig. 2. Phase diagram of the acetanilide–SAN system showing the T_g and solubility curves.

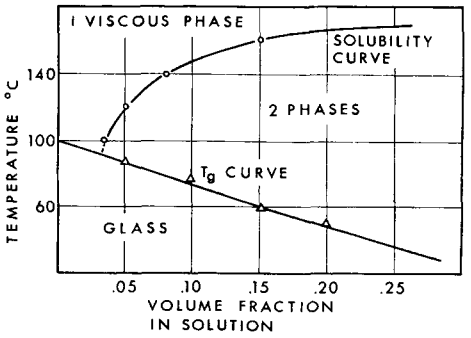

Fig. 3. Phase diagram of the anthracene–SAN system showing the T_g and solubility curves.

−63.5°C. Both values appear to be reasonable, although no data are available for comparison.

For anthracene, the experimental points fall nearly on a straight line. In terms of eq. (1), when $\alpha_f = \alpha_p$, the linear expression $T_g = V_p T_{gp} + V_f T_{gf}$ results. Fitting this equation to the data resulted in a T_{gf} of 44°C. for anthracene.

As expected, acetanilide is more efficient in lowering T_g because of its lower glass transition temperature. It is interesting to note that the empirical rule predicting a glass transition temperature at about 2/3 of the melting temperature for unsymmetrical polymers applies to the anthracene, but not to the acetanilide.

Solubility Curve. Figures 2 and 3 also display the equilibrium dissolved volume fraction of filler as a function of temperature. The curves for both systems flatten out while still below the melting point of the pure filler, indicating a marked degree of solid solubility in the concentration range studied.

The intersection of the solubility curve with the T_g curve represents the temperature at which maximum crystallization can occur (90°C. for the

anthracene and 68°C. for the acetanilide). Above this optimum temperature, the crystallization is limited by a thermodynamic solubility equilibrium; below the optimum, the glassy state is the crystallization barrier. The latter was checked by measuring T_g after complete crystallization at low temperatures. In all cases T_g was found to be equal to the crystallization temperature.

Figures 2 and 3 thus serve as phase diagrams which mark the boundaries between three states. Above the two curves, the system is one viscous liquid phase. Between the curves, the system is made up of two phases, a crystalline phase and a viscous liquid phase. Below the T_g curve, the polymeric matrix is in the glassy state containing dissolved filler, although filler crystals may also be present, depending on the prior thermal history.

Crystallization Kinetics

A primary concern in the fabrication of selectively crystallized composites is the rate at which the filler crystals are formed. Kinetic data also are helpful in the interpretation of crystal morphologies. In Figures 4 and 5 the sample crystallinity (volume fraction crystallized filler) has been plotted against time at several different crystallization temperatures for both systems. In the acetanilide system (Fig. 4) the initial volume fraction in solution was 0.30, while the initial dissolved fraction was 0.15 for the anthracene (Fig. 5).

In both systems the crystallization rate, as evidenced by the initial slope of the curves, increases to a maximum and then decreases as the

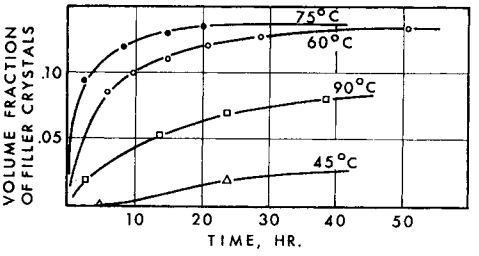

Fig. 4. Isothermal crystallization of acetanilide in SAN at various temperatures. The initial volume fraction in solution was 0.30.

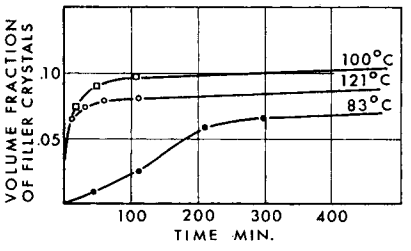

Fig. 5. Isothermal crystallization of anthracene in SAN at various temperatures. The initial volume fraction in solution was 0.15.

crystallization temperature is decreased. At first glance this suggests that the familiar competition between nucleation control (positive temperature coefficient) and diffusion control (negative temperature coefficient) is taking place, resulting in a maximum. However, when the crystallinity was plotted against the square root of time, a straight line resulted for all temperatures. This would imply that the crystal growth was diffusion-controlled at all temperatures if one assumes that the crystals grew unidirectionally with a constant concentration gradient. Electron micrographs showed that all the crystals did not grow unidirectionally; consequently, additional growth rate studies using hot-stage optical microscopy will be necessary to establish the limits of the diffusion controlled regime. As one might expect, the maximum crystallization rate and the maximum yield of crystals occur at nearly the same temperature.

Comparison of the two systems shows that anthracene crystallized considerably faster than acetanilide. This is expected, since the thermodynamic driving force ($T_{eq} - T_{cryst}$) for the anthracene was larger than that of the acetanilide in the temperature ranges investigated.

Filler Crystal Morphology

Electron micrographs of fracture-surface replicas from various composite samples are shown in Figures 6–11. They clearly reveal well-formed, low molecular weight crystals with a large variety of sizes and shapes. In

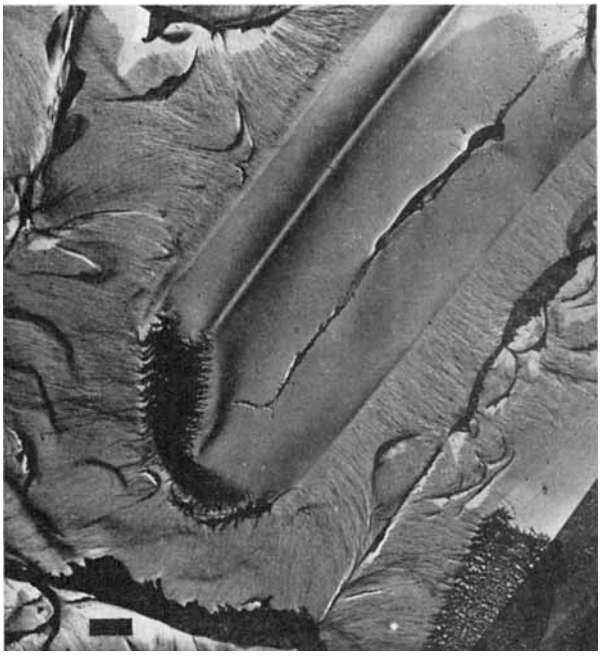

Fig. 6. Fracture surface of an acetanilide–SAN composite crystallized at 90°C. Note the apparently intact crystal–matrix interface. $V_{fc} = 0.12$. The scale bar represents 1 μ.

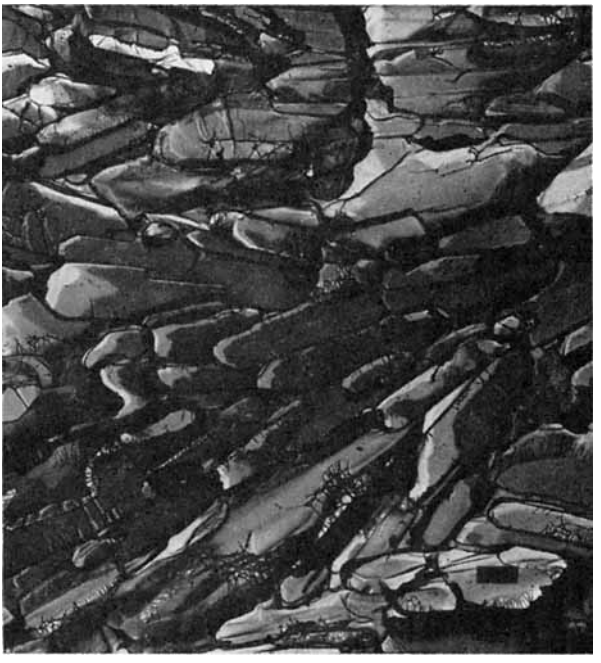

Fig. 7. Fracture of an acetanilide–SAN composite crystallized at 75°C. The crystals are smaller and more numerous than in Fig. 6. $V_{fc} = 0.18$. The scale bar represents 1 μ.

general, the bumpy polymer fracture surface is easily distinguished from the smooth crystal surfaces. The well-defined morphology of each sample depends on the heat treatment and crystallization temperature.

Acetanilide–SAN System. Fracture surfaces from acetanilide composites crystallized at 90, 75, 60, and 45°C. were examined. In all cases the initial dissolved filler volume fraction was 0.30. The final volume fraction of filler crystals (V_{fc}) was determined from the phase diagram under complete crystallization conditions.

At 90°C. (Fig. 6), large crystals have grown in an elongated rectangular shape whose ends often exhibit sharp crystallographic angles. The measurable aspect ratios vary from 2 to 10, with the length being about 20–50 μ and the width 5–20 μ. The shadow lengths and overlapping of crystals suggest a thickness which is considerably smaller than the width. The dark fibrous material visible on the left end of the crystal in Figure 6 is polymer which adhered to the crystal edge during fracture and then subsequently adhered to the replica. The bright ridge which runs the length of the crystal is more likely a wrinkle in the replica film and not a feature of the crystal itself. From the drawn appearance of the polymer the fracture was probably ductile in the matrix, while the faint fracture rings on the crystal surface indicate a brittle fracture through the filler. One important observation is that the crystal–matrix interface appears to be intact, indicating that adhesion is relatively good at the interface.

Crystals grown at 75°C. (Fig. 7) have about the same aspect ratio as those grown at 90°C. but are smaller and more numerous. The occasional dark lines stretching across the crystal from the edges are polymer threads which were drawn out during fracture.

At 60°C. (Fig. 8), the crystal morphology is considerably different from that of the previous samples. The crystals are highly branched dendritic bundles, each of which appears to have been nucleated at one point, from which growth occurred in all directions. Figure 9 shows a mixture of the two morphologies which resulted from a slow-cool crystallization. The

Fig. 8. Fracture surface of an acetanilide–SAN composite crystallized at 60°C. The crystals have a pronounced dendritic morphology. $V_{fc} = 0.17$. The scale bar represents 5 μ.

larger, more perfect crystals were formed at the higher temperatures, followed by dendritic growth which, in some cases, nucleated on the already grown large crystals.

When the crystallization temperature was lowered to 45°C., the morphology again changed significantly, as shown in Figure 10. Extremely long, thin, needlelike crystals with very little branching and high aspect ratios are predominant.

The replica observations were confirmed by observing actual fracture surfaces with scanning electron microscopy. The advantage of the replica technique lies in its higher resolution which allows more details to be seen at the interface.

Anthracene–SAN System. This system also exhibits three different types of crystals grown from an initially dissolved filler volume fraction of 0.20. At a crystallization temperature of 121°C. (Fig. 11), polygonal-shaped crystals have grown which measure between 1 and 2 μ across. Figure 11 illustrates a rather rare case where the fracture has propagated through the polymer matrix to the interface and then up over the crystal along the interface. The left edge of the crystal is protruding from the matrix, as evidenced by the bright shadow, and the majority of the crystal lies embedded in the matrix.

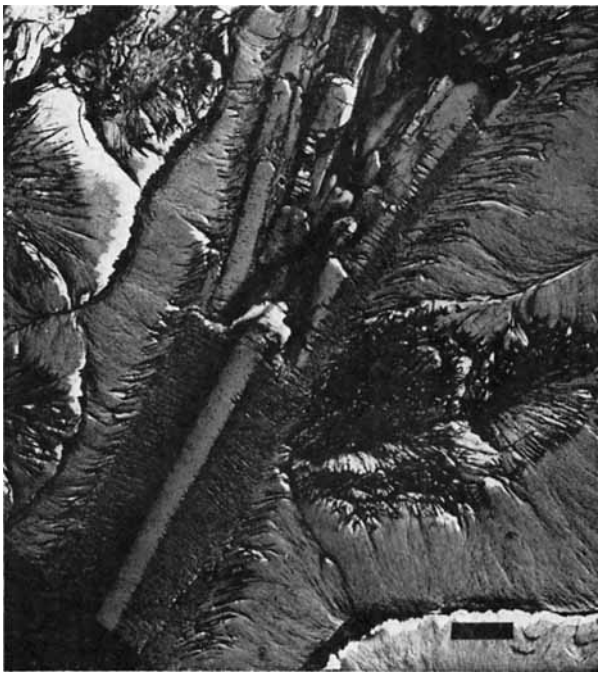

Fig. 9. Fracture surface of an acetanilide–SAN composite crystallized by slow cooling to 60°C. Both large crystals with dendritic overgrowth and dendritic bundles are present. $V_{fc} = 0.17$. The scale bar represents 1 μ.

At 100°C., dendritic bundles, very similar to the acetanilide dendrites, were the predominant morphology. At 83°C., long, thin, needlelike crystals grew with random distribution and orientation. The needles were very much like those grown at 45°C. in the acetanilide system, except that their average length was considerably shorter.

For both systems the filler crystals are larger and more perfectly shaped at the higher crystallization temperatures. As the temperature decreases, the crystals become smaller and more numerous. At still lower temperatures (38–45°C. above T_g of the matrix), both systems exhibit dendritic growth, presumably to aid in dissipating the heat of crystallization. When the crystallization temperature is lowered still further to 23–28°C. above

the matrix T_g, the viscosity of the matrix becomes very high and the crystallization becomes diffusion-controlled and very slow (see Figs. 4 and 5). Under these conditions dendritic growth is no longer needed to aid in removing the heat, and single, needlelike crystals result.

Fig. 10. Fracture surface of an acetanilide–SAN composite crystallized at 45°C. Long needle-shaped crystals with high aspect ratios are predominant. White areas are unshadowed regions. $V_{fc} = 0.17$. The scale bar represents 1 μ.

Mechanical Properties

The elastic modulus of a polymer filled with infinitely rigid spherical particles should be at least as great as that predicted by the limiting Kerner equation:[3]

$$\frac{G_0}{G_1} = 1 + \frac{15(1 - \nu_1)\, V_2}{(8 - 10\nu_1)\, V_1} \tag{2}$$

G_0 and G_1 are the shear moduli of the filled system and the unfilled polymer, respectively. The volume fractions of polymer and filler are given by V, and V_2, respectively, while the Poisson's ratio of the polymer is ν_1. Particles of other shapes generally increase the modulus even more than what is observed with spherical particles. If the modulus of the filler is not infinite but is comparable in magnitude to that of the matrix, the com-

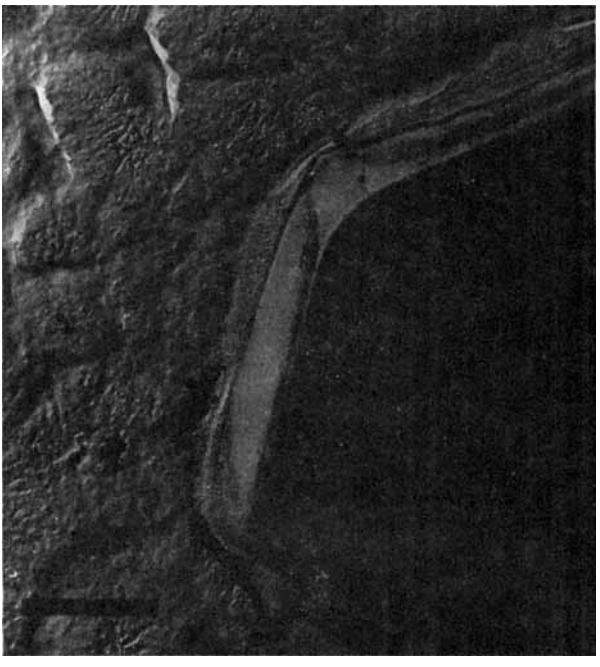

Fig. 11. Fracture surface of an anthracene–SAN composite crystallized at 121°C. The left edge of the crystal is protruding slightly, indicating fracture up over the crystal along the interface. $V_{fc} = 0.10$. The scale bar represents 0.5 μ.

posite modulus is less, and the more general form of the Kerner equation must be used for spheres:[4]

$$\frac{G_0}{G_1} = \frac{\dfrac{G_2V_2}{(7 - 5\nu_1)G_1 + (8 - 10\nu_1)G_2} + \dfrac{V_1}{15(1 - \nu_1)}}{\dfrac{G_1V_2}{(7 - 5\nu_1)G_1 + (8 - 10\nu_1)G_2} + \dfrac{V_1}{15(1 - \nu_1)}} \tag{3}$$

where G_2 is the shear modulus of the filler phase. In both of these equations it is assumed that there is good adhesion between the two phases.

Figures 12 and 13 show dynamic mechanical data measured on some of the SAN–acetanilide and SAN–anthracene systems. Dissolved acetanilide and anthracene plasticize the polymer, but if the curves are shifted on the temperature scale an amount equal to the difference in T_g between the filled and unfilled polymers, the shear modulus curves are essentially all superimposable. However, there is little indication that the organic crystals have increased the elastic modules. The crystallized systems contained crystal volume fractions of 0.18 and 0.38 in the case of acetanilide and 0.13 in the case of anthracene. If the shear moduli of the crystals were much greater (say 10 times or more) than that of the SAN polymer, the shear moduli should have increased at least 48 and 133% in the case of acetanilide and over 32% in the case of anthracene. The experimental

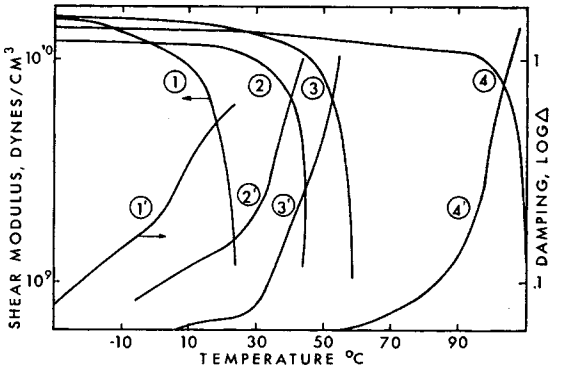

Fig. 12. Temperature variation of shear modulus and damping for samples having various crystal volume fractions of acetanilide. Primed curves indicated damping; unprimed curves indicate modulus: (*1*) $V_f = 0.30$, uncrystallized; (*2*) $V_{fc} = 0.18$; (*3*) $V_{fc} = 0.38$; (*4*) pure SAN.

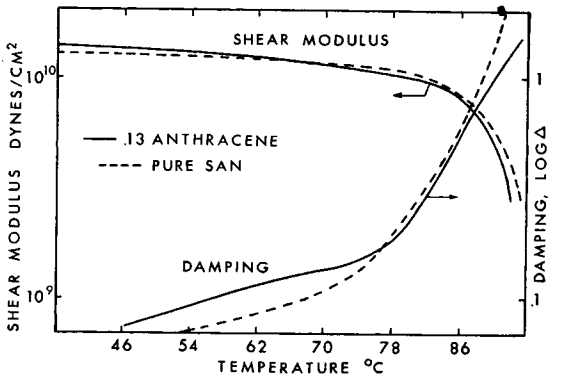

Fig. 13. Temperature variation of the shear modulus and damping for an anthracene–SAN composite ($V_{fc} = 0.13$) and a pure SAN sample. The pure SAN curves have been shifted 16°C. to the left for comparison.

results show no such increase. Since the electron microscope studies seem to indicate good adhesion between the phases, it can be assumed that the moduli of the organic crystals are approximately the same as that of SAN polymer in the glassy state.

However, if the filler phase is not spherical in shape but fibers or needles oriented perpendicular to the specimen faces (as electron microscope pictures tend to indicate), then the shear modulus G_L should be equal to or greater than what eq. (4) predicts:[5]

$$\frac{G_L}{G_1} = \frac{2G_2 - (G_2 - G_1)V_1}{2G_1 + (G_2 - G_1)V_1} \tag{4}$$

In this special case of oriented fibers, the shear modulus is less than what it would be if the filler particles were spheres. If the fibers have high

moduli compared to the polymer, the shear moduli should have increased at least 44 and 123% in the case of acetanilide and 30% in the case of anthracene as filler. Even after the SAN curve is shifted so as to compare the data at the same $(T_g - T)$ values, the observed increase in modulus is only 9% for the anthracene case at 38°C. For the acetanilide case, with 0.38 volume fraction of crystals, the experimental increase in shear modulus is 15% at −30°C. and 22% at 10°C. The modulus of the material containing 18 vol.-% acetanilide is actually less than that of pure SAN, even after the curves are shifted horizontally to compare at equal values of $(T_g - T)$. The error in the absolute value of the experimental moduli is estimated to be about 5%. Thus, even after picking the modulus data that show the greatest reinforcing action, it can be shown that the shear moduli of the crystals must be less than twice that of the SAN polymer.[4,6] Additional evidence that the elastic moduli of organic crystals is about 10^{10} dyne/cm.^{2} is found in recent measurements on polymer crystals; the elastic moduli in directions perpendicular to the polymer chains are essentially the same as the moduli of polymers in the glassy state.[7,8]

Elastic modulus measurements are not common on single crystals of organic materials. Many measurements, however, are available on materials which have strong bonding forces such as metals and ionic inorganic crystals where it is found that the moduli are ten to one hundred times as great as the moduli of polymers in the glassy state. Molecules in organic crystals and glassy polymers are both held together by the same type of weak van der Waals' forces, so it is not surprising that they both appear to have approximately the same moduli.

Thus, it is concluded that although high-modulus polymers cannot be appreciably stiffened by organic crystals, the technique of *in situ* crystallization provides good dispersion and control of the size and shape of the filler crystals and, as such, is a feasible method for fabricating composite materials.

The authors gratefully acknowledge support of this work by the Monsanto/Washington University ARPA Project under Office of Naval Research ONR Contract No. N00014-67-C-0218. We wish to thank Mr. W. McDonnell for the electron micrograph of the acetanilide–SAN composite crystallized at 45°C. (Fig. 10).

References

1. L. E. Nielsen, *Rev. Sci. Instr.*, **22**, 690 (1951).
2. F. Bueche, *Physical Properties of Polymers*, Interscience, New York, 1962, p. 117.
3. L. E. Nielsen, *Mechanical Properties of Polymers*, Reinhold, New York, 1962.
4. E. H. Kerner, *Proc. Phys. Soc. (London)*, **69B**, 808 (1956).
5. S. W. Tsai, National Aeronautics and Space Administration Report, NASA CR-71 (July, 1964).
6. C. Vander Poel, *Rheol. Acta*, **1**, 198 (1958).
7. I. Sakurada, T. Ito, and K. Nakamae, *Bull. Inst. Chem. Res. Kyoto Univ.*, **42**, 77 (1964).
8. I. Sakurada, T. Ito, and K. Nakamae, in *U.S.–Japan Seminar in Polymer Physics* (*J. Polymer Sci. C*, **15**), R. S. Stein and S. Onogi, Eds., Interscience, New York, 1966, p. 75.

Received September 21, 1967